

Lubricated Plane Slider Bearing: Analytic and Numerical Approach

*Original*

Lubricated Plane Slider Bearing: Analytic and Numerical Approach / Malvano, R; Vatta, Furio; Vigliani, Alessandro. - In: MECCANICA. - ISSN 0025-6455. - 34 (4):(1999), pp. 237-250. [10.1023/A:1004675126314]

*Availability:*

This version is available at: 11583/1406809 since:

*Publisher:*

*Published*

DOI:10.1023/A:1004675126314

*Terms of use:*

This article is made available under terms and conditions as specified in the corresponding bibliographic description in the repository

*Publisher copyright*

IEEE postprint/Author's Accepted Manuscript

©1999 IEEE. Personal use of this material is permitted. Permission from IEEE must be obtained for all other uses, in any current or future media, including reprinting/republishing this material for advertising or promotional purposes, creating new collecting works, for resale or lists, or reuse of any copyrighted component of this work in other works.

(Article begins on next page)

# Lubricated Plane Slider Bearing: Analytic and Numerical Approach

R. Malvano<sup>a</sup>, F. Vatta<sup>b</sup>, A. Vigliani<sup>b</sup>

<sup>a</sup> C.N.R. – Centro Studi Dinamica Fluidi  
Corso Duca degli Abruzzi, 24 – 10129 Torino – Italy

<sup>b</sup> Dipartimento di Meccanica - Politecnico di Torino  
C.so Duca degli Abruzzi, 24 - 10129 Torino - ITALY  
E-mail: [alessandro.vigliani@polito.it](mailto:alessandro.vigliani@polito.it)

**Keywords** tribology, lubrication, slider bearing

**Abstract** *For lubricated slider bearing the elementary theory of lubrication does not allow to describe the pressure build up at the entrance section.*

*In this work the whole flow field is subdivided into three regions: a first one, upstream of the entrance, where the fluid behaves like a perfect fluid; a second region, immediately downstream, where the two boundary layers gradually grow, extending up to a distance determined by means of a model based on analytic functions. The third region is described by Navier – Stokes, solved adopting a shooting method.*

*Numerical computations were carried out to determine the pressure distribution and the position of the center of pressure for different values of Reynolds number and pad angle.*

**Sommario.** *La teoria elementare della lubrificazione nel caso del pattino piano lubrificato non è in grado di evidenziare il fenomeno della sovrappressione nella sezione di ingresso.*

*Nel presente lavoro viene proposto un modello che suddivide il campo di moto in tre regioni: una prima a monte della sezione di ingresso, in cui il fluido si comporta come un fluido perfetto; una seconda regione immediatamente a valle, in cui si tiene conto del graduale sviluppo dello strato limite e la cui estensione è determinata tramite un modello basato sulle funzioni analitiche. La terza regione è studiata risolvendo l'equazione di Navier – Stokes con tecnica numerica basata su un metodo di shooting.*

*In questo lavoro viene riportato l'andamento della pressione all'interno del cuscinetto e la posizione del centro di pressione per differenti valori del numero di Reynolds e per varie inclinazioni del pattino.*

# 1 Introduction

The elementary theory of lubrication is based on a number of assumptions among which:

- the inertial effects are negligible;
- the over–pressure vanishes both at inlet and outlet sections.

These hypotheses hold only under well determined working conditions; to this concern, engineering practice owns a large literature reporting critical conditions that cause these hypotheses to fail, together with their effects on working characteristics.

The hypothesis of negligible inertial effects progressively loses validity with increasing velocities, that is with growing Reynolds number; consequently many authors were induced to develop new models to better represent the bearing actual behavior. Among the others, the works of Slezkin and Targ [1], Constantinescu [2] and Kahlert [3] appear to be relevant. These authors adopt the boundary conditions derived from the elementary theory and highlight the effect of convective terms on pressure distribution. The conclusions drawn from the analysis of these results lead to consider inertia relevant at high values of Reynolds number. However the results drawn from numerical solution of Navier–Stokes equation applied to plane slider bearings do not match these conclusions, thus proving that the proposed models are inadequate.

The hypothesis of zero over–pressure at inlet section simplifies the problem; however many researches dealing with fluid behavior around the entrance (Malvano and Vatta [4], Buckholtz [5], Tuck and Bentwick [6]) proved the existence of an over–pressure. Malvano et al. consider this over–pressure essentially due to the combined effects of the viscosity and of the free surface upstream of the inlet; other authors (Buckholtz [5], Tichy [7]) assume that the fluid is inertial upstream of the entrance, while it is viscous downstream: then they determine the inlet over–pressure by imposing constant flow rate.

To this extent it is evident that the slider bearing behavior cannot be accurately modeled without determining both the inlet over–pressure and the flow field of an inertial – viscous fluid.

This flow field can be modeled with Navier–Stokes equation, that is a nonlinear elliptical equation. Applying the hypothesis of small fluid film thickness, it yields a single fourth order partial differential equation in the stream function. By means of a finite differences method, the problem can be reduced to the solution of a system of four first order ordinary differential equations, with given boundary conditions both on the pad and on the slider: the solution at any section is completely determined when the stream function is known in the upstream section. Therefore, if the flow field at entrance is known, it can also be determined for all downstream sections by means of a *step by step* method.

As a matter of fact, the main difficulty in modeling the actual behavior of a slider bearing lies exactly in determining the flow field around the entrance.

Therefore, the aim of the present work is firstly to determine the influence of the geometric discontinuity at entrance and secondly to propose a simplified model to represent the transition taking place in the aforesaid region. To this aim, for a length  $\bar{x}^*$  downstream of the inlet section we determine the pressure gradient taking into account the gradual development of the boundary layer caused by the presence of a fixed wall (the pad) and of a moving one (the guide).

Therefore the whole flow field can be described with three different regions: a region upstream of the entrance, a transition region and finally the region inside the slider bearing, where the boundary layer is fully developed.

## 2 Analysis of entrance region

The inlet section is a geometrical discontinuity; it generates perturbations that propagate both upstream and downstream of the entrance. The aim of this section is to determine, at least qualitatively, the extension of this region. To simplify this complex problem, we refer to the model shown in Fig.1: the pad is assumed to be a semi–infinite wall (plane problem) parallel to the guide. This hypothesis is reasonable since the tilting angle is so small that it has negligible influence on thickness variations in this region.

The governing equation of a two–dimensional, incompressible, steady flow at constant viscosity, under the assumption that inertial effects can be neglected, can be expressed as follows:

$$\vec{\nabla}P = -2\mu\vec{\nabla} \times \vec{\omega} \quad (1)$$

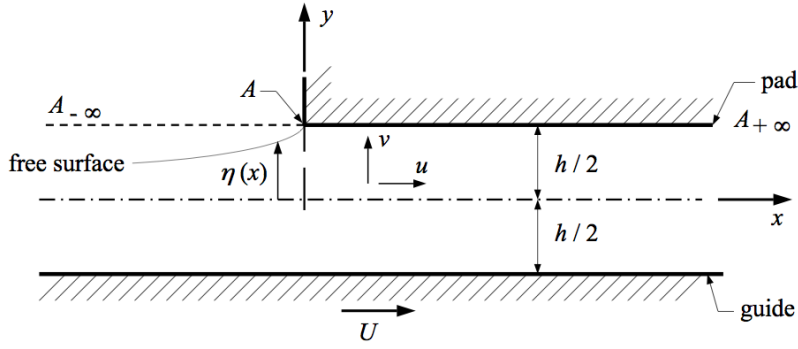


Figure 1: Plane slider bearing geometry

where

$$\vec{\omega} = \frac{1}{2} \left( \frac{\partial v}{\partial x} - \frac{\partial u}{\partial y} \right) \vec{k}$$

Letting

$$\mathcal{P} = \frac{P}{2\mu} = \frac{p - p_\infty}{2\mu} \quad \text{and} \quad \Omega = -\omega$$

we get the following Cauchy–Riemann differential equations:

$$\begin{cases} \frac{\partial \mathcal{P}}{\partial x} = \frac{\partial \Omega}{\partial y} \\ \frac{\partial \mathcal{P}}{\partial y} = -\frac{\partial \Omega}{\partial x} \end{cases} \quad (2)$$

Therefore,  $\mathcal{P}$  and  $\Omega$  are respectively the real and imaginary part of the function  $W$  in the complex variable  $z$ . According to the geometry above described, we can approximate the free surface with half-line  $AA_{-\infty}$ . The boundary conditions associated to equation (1) are:

$$\begin{cases} z = x + i h/2 & x \leq 0 & \mathcal{P} = -(\partial u / \partial x) \\ z = x + i h/2 & x \geq 0 & u + i v = 0 \\ z = x - i h/2 & -\infty \leq x \leq \infty & u + i v = U \end{cases} \quad (3)$$

where the first condition follows from the equilibrium in  $y$ -direction of a generic fluid element belonging to the free surface.

It is worth noting that the presence of viscosity alone justifies the existence of the inlet pressure build-up, in contrast with the elementary theory hypotheses; as a matter of fact, in the neighborhood of the stagnation point  $A$ , for  $x < 0$ ,  $\partial u / \partial x$  is negative. Therefore necessarily  $p - p_\infty$  must be positive.

In order to determine the flow field, we apply Schwarz's formula [8], which allows to calculate the function  $W(z)$  (apart from a purely imaginary constant) when the values of its real part are given on the border of the area: therefore  $\mathcal{P}$  and  $\Omega$  are determined inside a strip of the plane through the values assumed by the pressure on the walls delimiting the strip itself. Schwarz's formula relative to the strip (see Appendix A) is given by the following expression:

$$\begin{aligned} W(z) = & \frac{1}{2\pi} \left\{ \int_{-\infty}^{\infty} [f(X_1) + g(X_1)] \frac{\Theta}{\Phi} dX_1 - i [a \sinh(X) + b \cosh(X)] \cdot \right. \\ & \left. \int_{-\infty}^{\infty} [f(X_1) - g(X_1)] \frac{\Theta}{\cosh(X_1) \Phi} dX_1 \right\} - i K_o \end{aligned} \quad (4)$$

where

$$X = \frac{\pi x}{h} \quad X_1 = \frac{\pi x_1}{h} \quad Y = \frac{\pi y}{h} \quad a = \cos(Y) \quad b = \sin(Y)$$

$$\Phi(X_1, X, Y) = a^2 \cosh^2(X_1 - X) + b^2 \sinh^2(X_1 - X)$$

$$\Theta(X_1, X, Y) = a \cosh(X_1 - X) + i b \sinh(X_1 - X)$$

Therefore pressure  $P$  is given by the following expression:

$$P(X, Y) = \frac{\mu}{\pi} \left\{ a \int_{-\infty}^{\infty} [f(X_1) + g(X_1)] \frac{\cosh(X_1 - X)}{\Phi} dX_1 + a b \int_{-\infty}^{\infty} [f(X_1) - g(X_1)] \frac{dX_1}{\Phi} \right\}$$

In the present case, assuming that the fluid film thickness is constant, according to the elementary theory of lubrication the pressure is also a constant, its value being  $p_{\infty}$ ; therefore we can assume:

$$f(X) = \bar{f} + \epsilon_1(X) \quad g(X) = \bar{g} + \epsilon_2(X)$$

where  $\epsilon_1(X)$  and  $\epsilon_2(X)$  are small and hence negligible with respect to the mean values  $\bar{f}$  and  $\bar{g}$ . On the upper boundary, due to the discontinuity caused by the presence of the pad, it is necessary to assume two different constant values; a similar procedure is applied on the lower boundary. Assuming:

$$x < 0 \quad f(X_1) = f_1 \quad g(X_1) = g_1 \quad x > 0 \quad f(X_1) = f_2 \quad g(X_1) = g_2$$

it yields

$$P(X, Y) = \frac{\mu}{\pi} \{ a(f_1 + g_1) I_1 + a(f_2 + g_2) I_2 + a b(f_1 - g_1) I_3 + a b(f_2 - g_2) I_4 \} \quad (5)$$

where

$$I_1 = \int_{-\infty}^0 \frac{\cosh(X_1 - X)}{\Phi} dX_1 \quad I_2 = \int_0^{\infty} \frac{\cosh(X_1 - X)}{\Phi} dX_1 \quad I_3 = \int_{-\infty}^0 \frac{dX_1}{\Phi} \quad I_4 = \int_0^{\infty} \frac{dX_1}{\Phi}$$

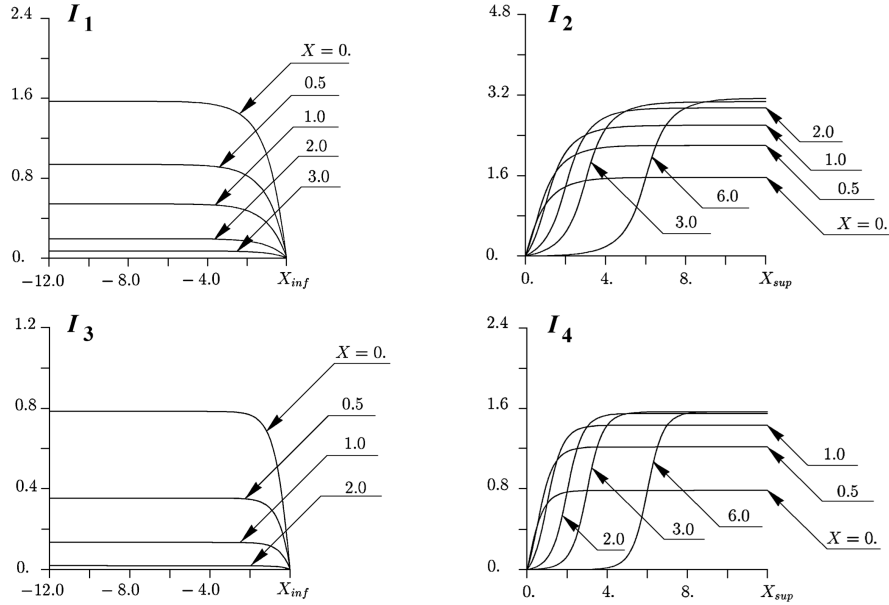


Figure 2: Plot of the integrals of eq.(5)

Figure 2 plots integrals  $I_1$ ,  $I_2$ ,  $I_3$ ,  $I_4$ , computed at  $Y = 0.25$  and at different values of  $X$ , versus lower and upper integration limits (respectively  $X_{inf}$  [ $I_1$  and  $I_3$ ] and  $X_{sup}$  [ $I_2$  and  $I_4$ ]).

From the analysis of these plots, it is possible to draw the following conclusions:

- for each integral there exists a finite integration limit whose growth does not affect the value of the integral itself (which remains constant). This limit models the condition at infinity;

- the distance where the disturbance due to the geometrical singularity vanishes is of the same order of the fluid film thickness;
- the region upstream of the entrance has small influence on the fluid field inside the lubricated pair.

Finally, the simplified model sketched in fig.3 can be adopted; it consists of three main regions:

- the first one, starting from infinite upstream and extending up to the inlet section, where the fluid can be regarded as a perfect fluid (pressure and velocity follow Bernoulli's law);
- a transition region, consisting of a "core" of inviscid flow inside the two boundary layers attached respectively to the guide and to the pad; moving downstream, the two boundary layers grow, progressively reducing the inviscid fluid "core". At a distance  $\tilde{x}^*$  the flow completely loses the characteristics of a perfect fluid; it is worth while to emphasize that in any section the pressure is constant;
- a third region where the fluid is both inertial and viscous.

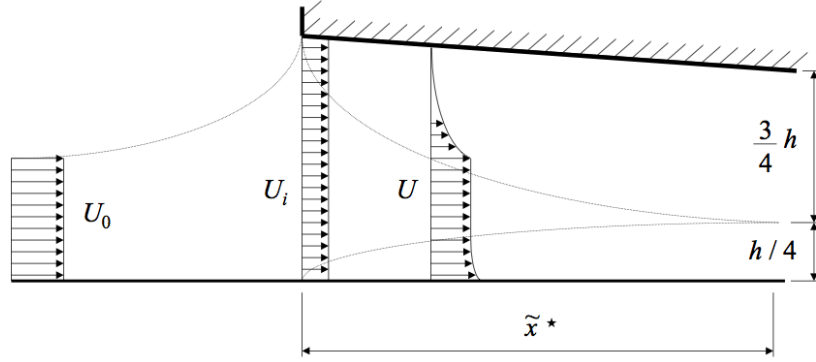


Figure 3: Model of the flow field

To determine the pressure distribution inside region **b)**, we assume the boundary layer thickness  $\delta$  of the pad to be similar to that due to a flat plate. Therefore the well known Blasius's relation holds:

$$\delta = h \Gamma \sqrt{\tilde{x}} \quad \text{where:} \quad \Gamma = 5 \frac{L/h}{\sqrt{\text{Re}}} \quad , \quad \text{Re} = \frac{U_o L}{\nu} \quad \text{and} \quad \tilde{x} = \frac{x}{h}$$

With no boundary layer due to the moving surface, the boundary layer of the fixed wall grows up to the thickness  $\delta = h$  at a distance  $\tilde{x}^*$ . It yields:

$$\delta = h \Gamma \sqrt{\tilde{x}^*} = h \quad \Rightarrow \quad \tilde{x}^* = \frac{1}{\Gamma^2}.$$

If the boundary layer of the moving surface behaved like that of the fixed wall, then, for symmetry reasons, the two layers would meet at  $y = h/2$ . Hence we would get:

$$\delta = h \Gamma \sqrt{\tilde{x}^*} = \frac{h}{2} \quad \Rightarrow \quad \tilde{x}^* = \frac{1}{4\Gamma^2}.$$

As a matter of fact, the boundary layer due to the moving surface grows more slowly than that due to the fixed wall: while on the fixed surface the longitudinal pressure gradient is negative (Malvano e Vatta [4]), on the moving wall the longitudinal pressure gradient is positive, hence the boundary layer grows more slowly. Therefore the two boundary layers meet at  $y = k h$ ; the value of constant  $k$  can be determined by means of the following expression:

$$\delta = h \Gamma \sqrt{\tilde{x}^*} = k h \tag{6}$$

We can now state as follows: for very low Reynolds (i.e.  $\leq 10^4$ ), the results shown in Fig.2 hold: the transition region extends downstream of the entrance up to a distance  $X \approx 2$  ( $\tilde{x}^* \approx 0.6$ ).

From eq.(6), for the same Reynolds number, we get  $k \approx 3/4$ . Under the hypothesis that such value holds also for larger Reynolds, it is possible to determine the value of  $\tilde{x}^*$  corresponding to the length of region **b**). From the continuity equation, under the assumptions that the velocity distribution inside the boundary layer is linear and that the fluid film thickness is constant (the last hypothesis is acceptable because of the very small value of the pad angle), we have:

$$\frac{3}{4}U_i h = U \left( \frac{3}{4}h - \delta \right) + \frac{1}{2}U \delta,$$

which allows to determine the velocity distribution inside the inviscid “core” as follows:

$$\frac{U}{U_i} = \frac{1}{1 - \frac{2\delta}{3h}} \cong 1 + \frac{2\delta}{3h}.$$

Applying Bernoulli’s equation, we get:

$$\bar{p} = \bar{p}_i - \frac{2}{3}\beta^2 \Gamma \sqrt{\tilde{x}} \quad \text{where:} \quad \beta = U_i/U_o$$

Finally, the longitudinal pressure gradient in the transition region is given by

$$\frac{d\bar{p}}{d\tilde{x}} = -\frac{1}{3} \frac{\beta^2 \Gamma}{\sqrt{\tilde{x}}} \quad \text{where:} \quad \bar{p} = \frac{p}{\rho U_o^2} \quad (7)$$

### 3 Analysis of the region downstream of entrance

In the region we are now considering the boundary layer height equals the fluid film thickness. In this flow field, Navier – Stokes equation for a two – dimensional incompressible flow at constant viscosity can be expressed by means of the stream function  $\psi$  as:

$$\psi_y \nabla^2 \psi_x - \psi_x \nabla^2 \psi_y = \nu \nabla^4 \psi. \quad (8)$$

For lubricated plane slider bearings the variation in the  $x$  direction can be neglected with respect to that in the  $y$  direction; therefore we get:

$$\psi_y \psi_{xyy} - \psi_x \psi_{yyy} = \nu \psi_{yyy}. \quad (9)$$

Let us introduce the following non dimensional variables:

$$\bar{\psi} = \frac{\psi}{Q} \quad \bar{y} = \frac{y}{h(x)} \quad \bar{x} = \frac{x}{L}$$

where  $Q$  is the lubricating flow rate,  $h(x)$  is the fluid film thickness and  $L$  is the pad length. Hence expression (9) can be rewritten in the form:

$$\frac{\partial \bar{\psi}}{\partial \bar{y}} \frac{\partial^3 \bar{\psi}}{\partial \bar{x} \partial \bar{y}^2} - \frac{\partial \bar{\psi}}{\partial \bar{x}} \frac{\partial^3 \bar{\psi}}{\partial \bar{y}^3} - \frac{2}{h(\bar{x})} \frac{dh}{d\bar{x}} \frac{\partial \bar{\psi}}{\partial \bar{y}} \frac{\partial^2 \bar{\psi}}{\partial \bar{y}^2} = \frac{\nu L}{h(\bar{x}) Q} \frac{\partial^4 \bar{\psi}}{\partial \bar{y}^4} \quad (10)$$

The flow rate  $Q$  evaluated at entrance is given by:

$$Q = \int_0^{h_i} u_i dy = U_o h_i \beta \quad \text{where} \quad \beta = \frac{U_i}{U_o};$$

therefore the coefficient  $\frac{\nu L}{h(\bar{x}) Q}$  on the right hand side of eq.(10) becomes:

$$\frac{\nu L}{h(\bar{x}) Q} = \frac{1}{\text{Re}} \frac{L^2}{h(\bar{x}) h_i \beta} \quad (11)$$

By substitution we have:

$$\frac{\partial \bar{\psi}}{\partial \bar{y}} \frac{\partial^3 \bar{\psi}}{\partial \bar{x} \partial \bar{y}^2} - \frac{2}{h(\bar{x})} \frac{dh}{d\bar{x}} \frac{\partial \bar{\psi}}{\partial \bar{y}} \frac{\partial^2 \bar{\psi}}{\partial \bar{y}^2} - \frac{\partial \bar{\psi}}{\partial \bar{x}} \frac{\partial^3 \bar{\psi}}{\partial \bar{y}^3} = \frac{1}{\text{Re}} \frac{L^2}{h(\bar{x}) h_i \beta} \frac{\partial^4 \bar{\psi}}{\partial \bar{y}^4} \quad (12)$$

Derivatives in  $\bar{x}$  can be computed with a first-order accurate backward difference approximation:

$$\begin{aligned}\frac{\partial \bar{\psi}}{\partial \bar{x}} &= \frac{\bar{\psi}(\bar{x}, \bar{y}) - \bar{\psi}(\bar{x} - \Delta \bar{x}, \bar{y})}{\Delta \bar{x}} \\ \frac{\partial^3 \bar{\psi}}{\partial \bar{x} \partial \bar{y}^2} &= \frac{\frac{\partial^2 \bar{\psi}(\bar{x}, \bar{y})}{\partial \bar{y}^2} - \frac{\partial^2 \bar{\psi}(\bar{x} - \Delta \bar{x}, \bar{y})}{\partial \bar{y}^2}}{\Delta \bar{x}} \\ \frac{dh}{d\bar{x}} &= \frac{h(\bar{x}) - h(\bar{x} - \Delta \bar{x})}{\Delta \bar{x}}\end{aligned}$$

so that eq.(12) is now given by:

$$\begin{aligned}\frac{d^4 \bar{\psi}}{d\bar{y}^4} &= \frac{d\bar{\psi}}{d\bar{y}} Z(\bar{x}) \left[ \frac{d^2 \bar{\psi}(\bar{x}, \bar{y})}{d\bar{y}^2} - \frac{d^2 \bar{\psi}(\bar{x} - \Delta \bar{x}, \bar{y})}{d\bar{y}^2} \right] - \frac{d\bar{\psi}}{d\bar{y}} \frac{d^2 \bar{\psi}}{d\bar{y}^2} Z(\bar{x}) W(\bar{x}) + \\ &- \frac{d^3 \bar{\psi}}{d\bar{y}^3} Z(\bar{x}) [\bar{\psi}(\bar{x}, \bar{y}) - \bar{\psi}(\bar{x} - \Delta \bar{x}, \bar{y})]\end{aligned}\quad (13)$$

where:

$$Z(\bar{x}) = \frac{\text{Re } \beta}{\Delta \bar{x}} \frac{h(\bar{x}) h_i}{L^2} \quad (14)$$

$$W(\bar{x}) = 2 \frac{h(\bar{x}) - h(\bar{x} - \Delta \bar{x})}{h(\bar{x})}. \quad (15)$$

Letting:

$$\begin{aligned}\bar{\psi}_1(\bar{y}) &= \bar{\psi} & \bar{\psi}_2(\bar{y}) &= \frac{d\bar{\psi}}{d\bar{y}} & \bar{\psi}_3(\bar{y}) &= \frac{d^2 \bar{\psi}}{d\bar{y}^2} & \bar{\psi}_4(\bar{y}) &= \frac{d^3 \bar{\psi}}{d\bar{y}^3} \\ K_1 &= \frac{d^2 \bar{\psi}(\bar{x} - \Delta \bar{x}, \bar{y})}{d\bar{y}^2} & K_2 &= \bar{\psi}(\bar{x} - \Delta \bar{x}, \bar{y})\end{aligned}\quad (16)$$

equation (13) changes into the following system of first order ordinary differential equations:

$$\left\{ \begin{aligned}\frac{d\bar{\psi}_4}{d\bar{y}} &= \bar{\psi}_2 Z(\bar{x}) (\bar{\psi}_3 - K_1) - \bar{\psi}_4 Z(\bar{x}) (\bar{\psi}_1 - K_2) - \bar{\psi}_2 \bar{\psi}_3 Z(\bar{x}) W(\bar{x}) \\ &= f_4(\bar{\psi}_1, \bar{\psi}_2, \bar{\psi}_3, \bar{\psi}_4) \\ \frac{d\bar{\psi}_3}{d\bar{y}} &= \bar{\psi}_4 = f_3(\bar{\psi}_1, \bar{\psi}_2, \bar{\psi}_3, \bar{\psi}_4) \\ \frac{d\bar{\psi}_2}{d\bar{y}} &= \bar{\psi}_3 = f_2(\bar{\psi}_1, \bar{\psi}_2, \bar{\psi}_3, \bar{\psi}_4) \\ \frac{d\bar{\psi}_1}{d\bar{y}} &= \bar{\psi}_2 = f_1(\bar{\psi}_1, \bar{\psi}_2, \bar{\psi}_3, \bar{\psi}_4)\end{aligned}\right. \quad (17)$$

with the following boundary conditions:

$$\begin{bmatrix} 1 & 0 & 0 & 0 \\ 0 & 1 & 0 & 0 \\ 0 & 0 & 0 & 0 \\ 0 & 0 & 0 & 0 \end{bmatrix} \cdot \begin{bmatrix} \bar{\psi}_1(0) \\ \bar{\psi}_2(0) \\ \bar{\psi}_3(0) \\ \bar{\psi}_4(0) \end{bmatrix} + \begin{bmatrix} 0 & 0 & 0 & 0 \\ 0 & 0 & 0 & 0 \\ 1 & 0 & 0 & 0 \\ 0 & 1 & 0 & 0 \end{bmatrix} \cdot \begin{bmatrix} \bar{\psi}_1(1) \\ \bar{\psi}_2(1) \\ \bar{\psi}_3(1) \\ \bar{\psi}_4(1) \end{bmatrix} = \begin{bmatrix} 0 \\ \frac{h(\bar{x})}{h_i} \frac{1}{\beta} \\ 1 \\ 0 \end{bmatrix} \quad (18)$$

Among the numerical methods available, we chose a shooting method, namely Newton's method; in this way the original problem is reduced to the solution of an initial values problem.



If velocity distribution  $u_i$  at entrance is known, it is possible to determine  $\beta$ ,  $K_1(\bar{y})|_i$  and  $K_2(\bar{y})|_i$ , that are given by:

$$\beta = U_i/U_o \quad K_2(\bar{y})|_i = \bar{\psi} = \frac{y}{h_i} \quad K_1(\bar{y})|_i = \frac{\partial^2}{\partial \bar{y}^2} K_2|_i = 0$$

We can now evaluate the flow field at the downstream section of co-ordinate  $\Delta\bar{x}$ ; then, with a step-by-step technique, all the variables at any section can be determined. Appendix B briefly describes this method.

## 4 Computational strategy

Pressure distribution inside the slider bearing is determined in the following way: by means of Bernoulli's equation, inlet pressure can be written as a function of parameter  $\beta$ , so that we have:

$$\bar{p}_{in} = \frac{1 - \beta^2}{2}.$$

Then, given  $\beta$  a trial value, by applying the shooting method, it is possible to determine unknown values of the functions  $\psi_i$ , and, in particular, the value of  $\psi_4(0)$ . The meaning of this function is evident if we consider the momentum equation in the  $x$  direction, given by:

$$\psi_y \psi_{yx} - \psi_x \psi_{yy} = -\frac{1}{\rho} p_x + \nu (\psi_{yxx} + \psi_{yyy})$$

Vanishing at  $y = 0$  both the velocity  $v$  and the longitudinal gradient  $\partial u / \partial x$ , being  $\psi_{yxx} \ll \psi_{yyy}$ , the previous equation can be reduced to the form:

$$\frac{1}{\rho} \frac{dp}{dx} = \nu \frac{\partial^3 \psi}{\partial y^3} \quad (19)$$

which, in non dimensional form, becomes:

$$\frac{d\bar{p}}{d\bar{x}} = \frac{1}{\text{Re}} \frac{L^2}{h^2(\bar{x})} \frac{h_i}{h(\bar{x})} \beta \psi_4(0). \quad (20)$$

It is therefore evident the relation between  $\psi_4(0)$  and  $d\bar{p}/d\bar{x}$ .

Finally the solution of system (17), with the boundary conditions given in (18), allows to determine the distribution of  $d\bar{p}/d\bar{x}$ . Such values hold only in region **c**, while in region **b** gradient  $d\bar{p}/d\bar{x}$  has to be computed by means of expression (7). The pressure gradient inside the bearing is now fully determined. The pressure distribution on the pad can be computed by integration, the outlet boundary condition given as zero pressure build-up. In general, the value of inlet pressure obtained by integration is different from the trial value; it is then necessary to vary parameter  $\beta$  to reach convergence.

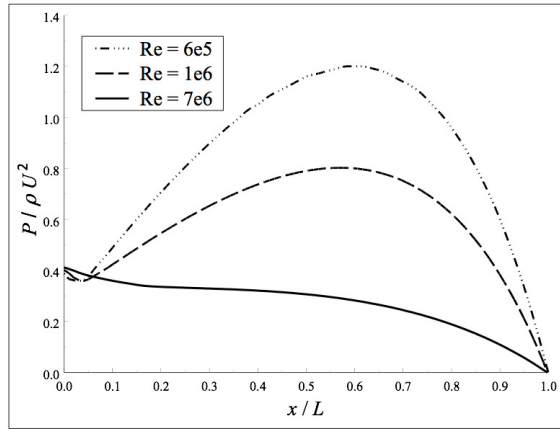


Figure 4: Pressure distribution for a linear slide bearing with thickness ratio  $h_i/h_e = 1.6667$

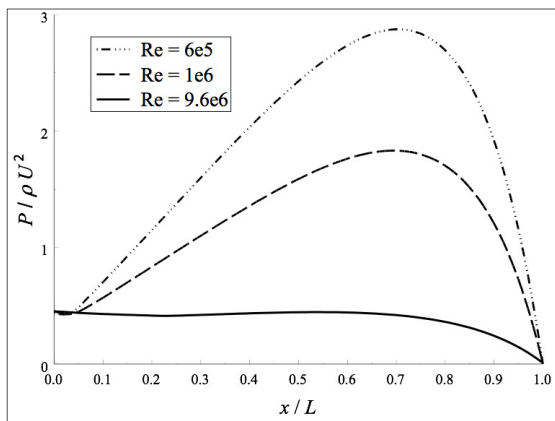


Figure 5: Pressure distribution for a linear slide bearing with thickness ratio  $h_i/h_e = 2.5$

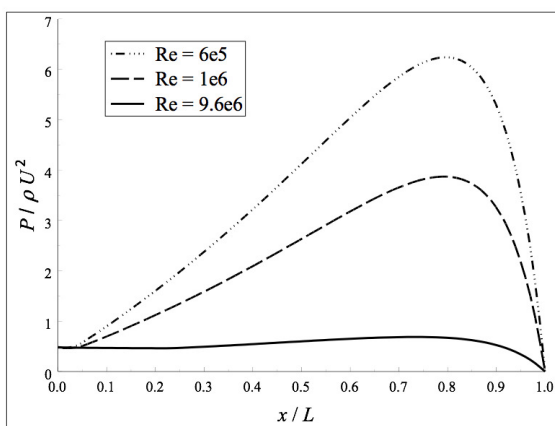


Figure 6: Pressure distribution for a linear slide bearing with thickness ratio  $h_i/h_e = 4.0$

## 5 Analysis of results and conclusions

Figures 4÷6 show the pressure distribution inside the bearing at different Reynolds numbers; this three plots are obtained for three different values of the ratio between inlet and outlet thickness (i.e.  $h_i/h_e$ ). It is worth noting that inlet pressure different from 0 implies a load capacity greater than the one obtained from the lubrication elementary theory. It can be observed that the non dimensional pressures decreases with growing Reynolds numbers (on the contrary the actual pressure grows with Re). Moreover non dimensional pressure at entrance is constant with increasing Reynolds numbers: therefore also inlet pressure grows with Re.

Now, let us examine the pressure behavior in the neighborhood of the inlet section: in this region pressure initially decreases along the bearing; then, when transient is over, pressure rises up to its maximum value and successively decreases again to meet the outlet boundary conditions.

From the analysis of the results it can be stated that the inlet pressure increase is due both to Reynolds number and to the pad angle.

Beyond these results, the proposed numerical technique allows to evaluate the reliability of the analytical methods developed by different Authors to determine pressure distribution when inertial terms in the equation of motion are not neglected. Among the Authors that studied this problem, it is worth mentioning Slezkin and Targ [1], Kahlert [3] and Constantinescu [2]. Slezkin and Targ propose a method known as *mediate inertia*, which basically consists in substituting the convective terms with their mean value. Kahlert uses a perturbation technique; finally Constantinescu assumes a velocity distribution that, though in presence of inertial terms, can be given by adding the Couette motion to the Poiseuille one.

Adopting as inlet values the velocity distribution and the longitudinal pressure gradient determined with the above approximate techniques, the results are practically coincident with those obtained adopting the exact method.

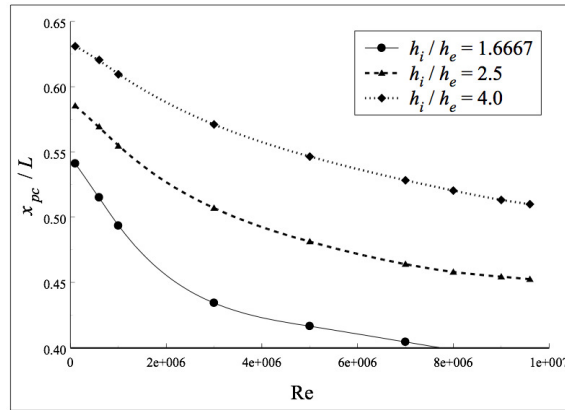


Figure 7: Pressure center  $x_{pc}$  versus Reynolds number

Finally, Fig.7 shows the position of the pressure center  $x_{pc} = \int_0^L px dx / \int_0^L p dx$  plotted against the Reynolds number for different ratios  $h_i/h_e$ . It is worth noting that the pressure center shifts upstream at increasing Re, thus explaining the bidirectional operation for a tilting pad bearing. In fact it is possible to determine operating conditions corresponding to  $x_{pc}/L = 0.5$ ; therefore the centrally pivoted pad satisfies the conditions to reverse motion direction.

As a conclusion, we can state that the proposed analytic – numerical method can be applied to the analysis of a lubricated plane slide bearing, in presence of a very complex phenomenon, such as the inlet transient. The inlet pressure build – up causes both load capacity to increase and the pressure force resultant to shift towards the inlet section.

## References

- [1] Slezkina N.A., Targ S.M., *L'Equazione Generalizzata di Reynolds*, Accad. Sc. U.R.S.S., **54** (3), 1946.
- [2] Constantinescu V.N., *On the possibilities of improving the accuracy of the evaluation of inertial forces in laminar and turbulent films*, A.S.M.E. Journal of Lubrication Technology, **96**, 1974, pp.69-79.
- [3] Kahlert W., *Der einfluss der tragheitskrafte bei der hydrodynamischen schmiermitteltheorie*, Ingenr. Arch., **16**, 1947, pp.321-342.
- [4] Malvano R., Vatta F., *Lubricated Plane Slider Bearing: Solution of the Inlet Problem with Upstream Free Surface*, J. Fluid Mech., **359**, 1998, pp.281-297.
- [5] Buckholz R. H., *The Effect of Lubricant Inertia Near the Leading Edge of a Plane Slider Bearing*, J. Trib., **109**, 1987, pp.60-64.
- [6] Tuck E. O., Bentwich M., *Sliding Sheets: Lubrication With Comparable Viscous and Inertia Forces*, J. Fluid Mech., **135**, 1983, pp.51-69.
- [7] Tichy J. A., Chen S. H. *Plane Slider Bearing Load Due to Fluid Inertia – Experiment and Theory*, J. Trib., **107**, 1985, pp.32-38.
- [8] Cisotti U., *Idromeccanica Piana*, Libreria Editrice Politecnica, Milano, **109**, 1921.

## Appendix A

Schwarz's formula for a circle of radius  $R$ , apart from a purely imaginary constant, has the following expression ([8]):

$$W(\zeta) = \frac{1}{2\pi} \int_0^{2\pi} \phi(\zeta) \frac{\bar{\zeta} + \zeta}{\bar{\zeta} - \zeta} d\bar{\sigma} \quad (21)$$

where:

- $\phi$  is the real part of analytical function  $W(\zeta)$  on the circle boundary;
- $\bar{\zeta} = R e^{i\bar{\sigma}}$ ;
- $\zeta = R e^{i\sigma}$ ;
- $0 \leq r \leq R$ .

For a strip of height  $h$ , eq.(21) must be modified by means of the following conformal mapping:

$$\zeta = \tanh \frac{\pi z}{2h} = \tanh \frac{\pi x \pm i y}{2h}$$

$$\bar{\zeta} = \tanh \frac{\pi \bar{z}}{2h} = \tanh \frac{\pi x \pm i h/2}{2h}$$

Let  $d\bar{\sigma} = d\bar{\zeta}/\bar{\zeta}$ ; then eq.(21) has the form (4), where  $f$  and  $g$  are the real part of function  $W$  on the strip upper and lower border respectively.

## Appendix B

Let us consider the following system of ordinary differential equations:

$$\begin{cases} y'_1 = f_1(t, y_1, y_2, y_3, y_4) \\ \vdots \\ y'_4 = f_4(t, y_1, y_2, y_3, y_4) \end{cases} \quad (22)$$

with the following boundary conditions:

$$\begin{cases} y_1(a) = k_1 & y_2(a) = k_2 \\ y_1(b) = k_3 & y_2(b) = k_4 \end{cases}$$

with  $a \geq t \geq b$ .

Consider now the following initial value problem:

$$\begin{cases} u'_1 = f_1(t, u_1, u_2, u_3, u_4) \\ \vdots \\ u'_4 = f_4(t, u_1, u_2, u_3, u_4) \end{cases} \quad (23)$$

with the boundary conditions:  $u_1(a) = s_1$ ;  $u_2(a) = s_2$ ;  $u_3(a) = s_3$ ;  $u_4(a) = s_4$ .

If

$$s_1 \equiv k_1 \quad \text{and} \quad [u_1(k_1, k_2, s_3, s_4)]_b \equiv k_3$$

$$s_2 \equiv k_2 \quad \text{and} \quad [u_2(k_1, k_2, s_3, s_4)]_b \equiv k_4$$

then the functions  $u_i$  coincide with the functions  $y_i$  and the boundary value problem (22) is substituted by initial value problem (23).

Let

$$\begin{cases} \phi_1(s_3, s_4) = [u_1(k_1, k_2, s_3, s_4)]_b - k_3 \\ \phi_2(s_3, s_4) = [u_2(k_1, k_2, s_3, s_4)]_b - k_4 \end{cases} \quad (24)$$

then the problem changes into the determination of the values of  $s_3$  and  $s_4$  such that both  $\phi_1$  and  $\phi_2$  vanish at point  $t = b$ . Let us call  $s_3$  and  $s_4$   $p_1$  and  $p_2$  respectively: they are system parameters and can be determined with iterative technique, applying Newton's method.

We get the system:

$$\begin{cases} \left( \frac{\partial u_1}{\partial p_1} \right)^r (p_1^{r+1} - p_1^r) + \left( \frac{\partial u_1}{\partial p_2} \right)^r (p_2^{r+1} - p_2^r) = -(\phi_1)^r \\ \left( \frac{\partial u_2}{\partial p_1} \right)^r (p_1^{r+1} - p_1^r) + \left( \frac{\partial u_2}{\partial p_2} \right)^r (p_2^{r+1} - p_2^r) = -(\phi_2)^r \end{cases} \quad (25)$$

that allows to determine the parameters  $p_i$  at iteration “ $r + 1$ ” if the same parameters are known at iteration “ $r$ ”. Coefficients  $(\partial u_i / \partial p_j)^r$  can be computed from the following system:

$$\begin{vmatrix} \frac{\partial u'_1}{\partial p_1} & \frac{\partial u'_1}{\partial p_2} \\ \cdot & \cdot \\ \cdot & \cdot \\ \frac{\partial u'_4}{\partial p_1} & \frac{\partial u'_4}{\partial p_2} \end{vmatrix} = \begin{vmatrix} \frac{\partial f_1}{\partial u_1} & \dots & \frac{\partial f_1}{\partial u_4} \\ \cdot & & \cdot \\ \cdot & & \cdot \\ \frac{\partial f_4}{\partial u_1} & \dots & \frac{\partial f_4}{\partial u_4} \end{vmatrix} \begin{vmatrix} \frac{\partial u_1}{\partial p_1} & \frac{\partial u_1}{\partial p_2} \\ \cdot & \cdot \\ \cdot & \cdot \\ \frac{\partial u_4}{\partial p_1} & \frac{\partial u_4}{\partial p_2} \end{vmatrix} \quad (26)$$

Being

$$\frac{\partial}{\partial p_j} \left( \frac{du_i}{dt} \right) = \frac{d}{dt} \left( \frac{\partial u_i}{\partial p_j} \right) = \frac{d}{dt} U_{i,j}$$

we have:

$$\begin{vmatrix} U'_{11} & U'_{12} \\ \cdot & \cdot \\ \cdot & \cdot \\ \cdot & \cdot \\ U'_{41} & U'_{42} \end{vmatrix} = \begin{vmatrix} \frac{\partial f_1}{\partial u_1} & \dots & \frac{\partial f_1}{\partial u_4} \\ \cdot & & \cdot \\ \cdot & & \cdot \\ \frac{\partial f_4}{\partial u_1} & \dots & \frac{\partial f_4}{\partial u_4} \end{vmatrix} \begin{vmatrix} U_{11} & U_{12} \\ \cdot & \cdot \\ \cdot & \cdot \\ \cdot & \cdot \\ U_{41} & U_{42} \end{vmatrix} \quad (27)$$

with the following boundary conditions:

$$\begin{vmatrix} U_{11} & U_{12} \\ U_{21} & U_{22} \\ U_{31} & U_{32} \\ U_{41} & U_{42} \end{vmatrix} \underset{a}{=} \begin{vmatrix} 0 & 0 \\ 0 & 0 \\ 1 & 0 \\ 0 & 1 \end{vmatrix} \quad (28)$$

When coefficients  $U_{i,j}$  are determined, system (25) becomes:

$$\begin{cases} U_{1,1}(b) \cdot (p_1^{r+1} - p_1^r) + U_{1,2}(b) \cdot (p_2^{r+1} - p_2^r) = k_3 - u_1^r(b) \\ U_{2,1}(b) \cdot (p_1^{r+1} - p_1^r) + U_{2,2}(b) \cdot (p_2^{r+1} - p_2^r) = k_4 - u_2^r(b) \end{cases}$$

hence it is possible to compute the increments to  $(p_1^r)$  and to  $(p_2^r)$ .

Integrating system (23) with these new initial conditions we get the value of errors:

$$\varepsilon_1^{r+1} = k_3 - u_1^{r+1}(b) \quad \varepsilon_2^{r+1} = k_4 - u_2^{r+1}(b).$$

If convergence is not reached, the method goes on computing new increments  $\delta p_1$  e  $\delta p_2$ .